

Simulation of the channelling of ions from MeV C₆₀ in crystalline solids*

A Fetterman¹, L Sinclair¹, N Tanushev¹, T Tombrello¹ and E Nardi²

¹ Basic and Applied Physics, California Institute of Technology, Pasadena, CA, USA

² Department of Particle Physics, Weizmann Institute of Science Rehovot, 76100, Israel

E-mail: tat@its.caltech.edu

Received 18 March 2007, in final form 23 April 2007

Published 18 May 2007

Online at stacks.iop.org/JPhysB/40/2055

Abstract

Simulations were performed describing the motion and breakup of energetic C₆₀ ions interacting with crystalline targets. A hybrid algorithm was used that employs a binary collision model for the scattering of the carbon ions by the atoms of the solid, and molecular dynamics for the Coulomb interactions of the 60 carbon ions with one another. For the case of yttrium iron garnet (YIG), directions such as [1 1 0], [1 0 0], [0 1 0] and [0 0 1] demonstrate channelling for a large fraction of the C ions. For directions such as [1 1 1], [2 1 1] and [7 5 3] the trajectories show no more channelling than for random directions. The effects of tilt, shielding and wake-field interactions were investigated for YIG and α -quartz.

1. Introduction

When an energetic ion enters a lattice close to a major axial direction, it undergoes a set of correlated small-angle collisions that tend to ‘channel’ its motion so as to avoid close collisions with lattice atoms. The motion becomes channelled because the projectile will be slightly deflected by the repulsive potential of the first atom, then again by the second until the ion moves nearly parallel to the atomic string (1). This causes the number of scattered ions to be significantly diminished, as more of the ions remain in the channel and penetrate further into the crystal than into an amorphous solid of the same composition. By learning more about this process, we can also understand much more about track damage in crystals by heavy ions, discover more about the properties of ions travelling through matter, in particular through an electron gas, and also provide new methods to probe a crystal for impurities [1].

The same phenomenon persists if a molecular or cluster ion is employed, but the interactions become much more complex. The cluster of ions undergoes Coulomb explosion upon impact, as each ion sees the repulsive charge of its neighbouring ions. These lateral

* Supported in part by the National Science Foundation (grant no. DMR97-30893).

forces can bring about the expansion and disruption of the cluster and oppose small-angle scatterings with the lattice atoms that channel the ions. The ions move through the material much faster than the lattice can react, so we can treat the lattice as fixed. Because there have been observations of cluster-ion-induced damage in YIG ($\text{Y}_3\text{Fe}_5\text{O}_{12}$) [2] and α -quartz [3], we consider here only these materials. We use energies ranging from 10 to 40 MeV or about 166 to 667 keV per atom. These energies have also been realized experimentally [2].

One major reason for making the present study is to ascertain whether the cluster upon traversing the channel remains intact. This could be of importance in future applications, the purposes of which are to transport clusters to given targets using either crystalline materials or nanotubes. Another point worth mentioning is that the present calculation is performed by means of the two-body interaction between the projectile ions and the individual target atoms and not by using a continuous potential within the channel. This work also brings up interesting issues regarding the interaction of energetic ions with an electron gas, in particular charge state and screening. In part 2 we discuss theory and methods of computation, while in part 3 the results are presented. In part 4 we conclude and make recommendations for future experiments.

2. Theory and calculations

2.1. Molecular dynamics

In order to model the many inter-atomic interactions that take place while the cluster travels through the crystal, we apply separately (but self-consistently) the processes of binary collisions with lattice atoms and intra-cluster molecular dynamics. We use a predictor–corrector model as presented and carried out by Hartman *et al* [4, 5]. This procedure is appropriate for use in this regime because, as mentioned earlier, the response time of the lattice is very slow compared to the motion of the ions.

Molecular dynamics are resolved on a timescale shorter than that necessary for resolving binary collisions by the use of an adaptive time step. The adaptive time step works by taking successively smaller test time steps until the estimated velocity error test is passed. Once the molecular dynamics step is completed, the binary collision is carried out using the ‘magic formula’ of Biersack and Haggmark for momentum transfer [6]. This algorithm is at the core of the widely used TRIM code [7], and provides for a fast approximate solution to the scattering integral, by deriving the polar deflection angle ϑ . This angle is calculated on the basis of the impact parameter of the collision, as well as on the centre-of-mass energy, and on the binary interaction potential. The impact parameter is determined on the basis of the position of the lattice target atom and of the particle trajectory, while the potential used here is the Moliere approximation to the Thomas–Fermi interatomic potential [6]. Specifically, the calculation is based on the use of the ‘scattering triangle’. Denoting the impact parameter by p , the sum of the radii of curvature of the trajectories at closest approach by ρ , it follows that [6]

$$\cos(\vartheta/2) = (\rho + p + \delta)/(\rho + r_0), \quad (1)$$

where r_0 is the distance of closest approach and δ is a small correction term.

In principle, other potentials as well as other computational techniques could be employed. However, the current very widely used procedure adopted here is sufficient for our purposes. The process of multiple scattering in the electron gas, which constitutes the channel, was neglected, see discussion below.

Once the binary collision is carried out, the adaptive time step process is repeated, and so on. The transit time of the projectile through the 700 Å YIG target is of the order of 10^{-13} s.

From the vibrational spectra of C₆₀ [8], one obtains that the time of the normal vibrational mode of the molecule is of the order of 3×10^{-13} s. Hence, the time scales of both of these processes are of the same order of magnitude. However, the molecular configuration is disrupted after the cluster penetrates the first few target layers, with the outer binding electrons being stripped away almost immediately.

Following Hartman *et al* [4, 5], the potential describing the intra-cluster forces (used in the calculation of the molecular dynamics) is composed of a hard-core repulsion and Coulomb potential between the partially ionized cluster components. The latter component, the screened two-body Coulomb potential V_c , drives the Coulomb explosion as the cluster penetrates the target. It is given by the Yukawa potential [4]

$$V_c = (q_i q_j / r) \exp(-r/a), \quad (2)$$

where q_i and q_j are the charges of ions i and j , r the distance between them. The dynamic screening length a is given by $a = (v_p^2 + v_f^2)^{1/2} / \omega_p$, with v_p being the projectile velocity, v_f the valence electron Fermi velocity and ω_p the plasma frequency of the valence electron gas, the latter is proportional to the number of valence or ‘screening electrons’, see discussion below.

2.2. Ionic charge state

The charge state or ionization state of the penetrating ions driving the Coulomb explosion is complex. On the one hand, for ions moving within an amorphous material, basically equivalent to non-channelled ions, the charge state is given by the well-known Brandt charge as given in Ziegler *et al* [7]. On the other hand, channelling confines the trajectories of swift ions in a crystal to the open space between atomic rows where they only interact with the outer delocalized electrons, and hence the ions penetrate a medium approximating an electron gas [9–11]. Thus the charge exchange processes of electron capture and loss are mostly determined by the interaction between the ion and a quasi-free electron gas [9, 10].

The question arises however whether the charge state calculation for a single isolated ion could be applied to the cluster. This issue has been the topic of extensive experimental work by Brunelle *et al* [12] as well as theoretical analysis [13]. For C₁₀, the ionic charge state could be up to 30% less compared to that of the individual ionic charge state, at the initial stages of cluster penetration. No published data however exist for clusters of the order of 60 atoms. We have chosen to neglect this effect here, whose influence would be the reduction of the intra-cluster Coulomb repulsion and hence increasing the survival of the cluster within the channel.

For the cluster ions advancing within the channel, the issue of electron-induced ionization is non-trivial. The relative valence electron to ion velocity is determined by the ion velocity v_p and the valence electron Fermi velocity v_f and is given by $[v_p^2 + v_f^2]^{1/2}$, where v_f is based on the YIG valence electron density of $6.4 \times 10^{22} \text{ cm}^{-3}$. Adding both velocities gives an electron kinetic energy of 14.3 eV, the energy thus obtained surpasses the magnitude of the energy needed to ionize the outermost electron of the neutral carbon cluster constituent which is 9 eV. It is not likely that there will be further ionization of the C⁺¹ ion, the ionization energy of which is 29.2 eV. For projectile velocities approaching zero the effective electron kinetic energy, assuming all the valence electrons contribute to the Fermi velocity is 7 eV, not enough to ionize the neutral carbon. The Fermi velocity was calculated here as it was in [11], which deals with channelling studies in gold crystals. The value of the Fermi velocity calculated there was found to be consistent with the experimentally observed width of the dielectronic recombination line.

The ionization cross section can be approximated from the well-known Lotz formula, quoted and discussed in [14], which however was derived for dilute ideal plasmas. Applying this formula we obtain a cross section equal to 1.6×10^{-16} cm, giving a mean free path (m.f.p.) for ionization of about 10 Å. However, since we are dealing here with dense cold material, the ionization cross section could also be much reduced near threshold [14], making the m.f.p. for single ionization substantially longer (the thickness of the target in the calculation is 700 Å). We therefore conclude that the ionization state could attain a value of unity at some distance within the 700 Å target for the 10 MeV cluster. The preceding calculation is based on the assumption that the radiative recombination cross section within the channel is negligible, which is indeed the case for higher energy ions [9]. Assuming the ionic charge state of unity throughout the length of the channel is the most realistic charge state value that we could adopt under these conditions.

Employing the same reasoning to the 40 MeV cluster yields a charge state 2 which is attained within the channel. In this respect we note that it would be of great interest in this connection to measure the charge state of channelled individual and not clustered carbon ions, at the appropriate energies of 166 and 667 keV exiting thin YIG targets.

2.3. Screening and wake potential

Another issue detrimental to the Coulomb explosion process is the dynamic screening length defined above in connection with equation (1). Determining the number of screening electrons within the channel appropriate for the above calculation is not a trivial matter. One difficulty is that the electron gas in the channel is inhomogeneous [10]. However, we see no notable qualitative differences in our results if we suppose larger or smaller (homogenous) electron densities. One might expect inhomogeneities to be mitigated by the fact that the ions quickly track from side to side in the channel and so sample an average electron density. Calculating the electron velocity as above where the Fermi energy was accounted for, and assuming an electron density of 6.4×10^{22} within the channel, we obtain a screening length of 1.5 Å for the 10 MeV cluster. For the 40 MeV cluster a screening length of 2.5 Å was similarly calculated. The actual screening length could be longer than these values should not all channel electrons participate in the screening process. The screening length approximation is discussed in detail in [13], where a problem similar to the present one was treated.

We have also taken into account the effect of electron-wake potentials. The Coulomb explosion is not a complete description of the motion of the ions, as described by Gemmell *et al* [15]. There is also a wake effect pulling together the angular distribution of the ions, aligning them with the direction of motion. This effect was applied by using the potential given by Gemmell *et al* [15]:

$$\Phi(s, \rho) = -\frac{2Q}{a} \sin\left(\frac{s}{a}\right) K_0\left(\frac{\rho}{a}\right) \Theta(s), \quad (3)$$

where Q is the charge defined above, s is the distance from the particle parallel to its velocity vector, ρ is the distance from the particle perpendicular to that same vector, K_0 is the modified Bessel function of the second kind to the zeroth order, and $\Theta(s)$ is the Heaviside function. The potential was applied pairwise, with the forward member of the pair being the source of the potential and the rear member of the pair seeing its effects. This is not unreasonable for ions away from the centre of the cluster, but may overstate the effect for ions in the vicinity of other ions. There has not been much research into the effects of this electron wake on multiple ions in close proximity, and so this solution may be the best available. Although this treatment involves simplifying approximations, the effect as will be seen, using the simple form, is very

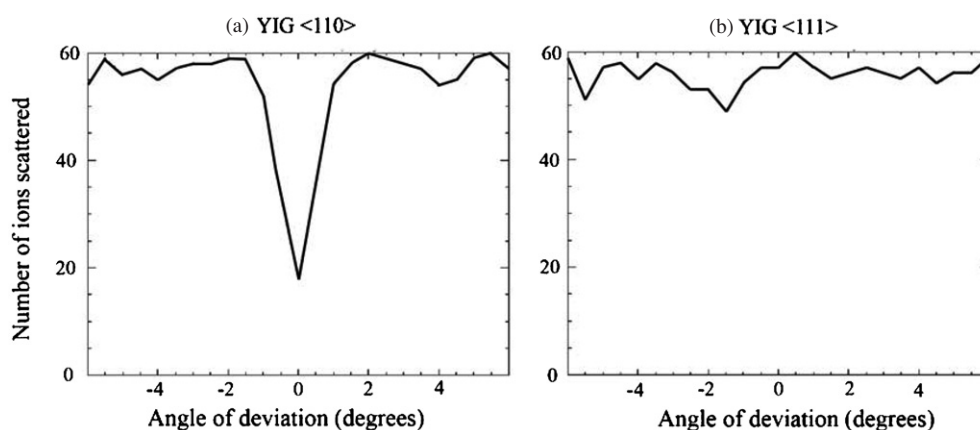


Figure 1. Dechannelling simulations, in (a) channelling, and (b) non-channelling directions. Ions outside of a 10 Å cylinder after 50 fs were counted for this simulation. These simulations are for 10 MeV clusters impacting on YIG.

small. Improving upon the model describing the wake potential would be hardly worthwhile due to the small effect.

An additional interaction term is the slowing of the ion due to drag from electrons or electronic stopping. This term was estimated by using tabulated TRIM calculations [7], although stopping by the quasi-electron gas within the channel is different from that for the bulk material. By using the tabulated values significant time is saved in calculation with negligible loss of accuracy. The effect of this term however is quite small.

3. Results

In the following we present results where 10 and 40 MeV C_{60} clusters are launched into YIG and quartz crystals in different initial directions and where the thickness of the crystal target is 700 Å. Before going further we would like to discuss the experimental consequences of the results. It would be difficult to make a free-standing crystal of one of these materials thin enough (~ 700 Å), such that a transmission experiment could be done for such low-energy carbon ions. For that reason we assumed that the first experiments that could be considered would be in a back-scattering geometry where the carbons that back scattered, i.e., had been dechannelled and then Rutherford scattered into a detector near 180° , would be observed. That way a very thick or epitaxially grown crystal could be used.

In order to output the results of the simulation into readable charts, we needed to develop analytic criteria for the definition of ‘channelled’ and ‘non-channelled’ ions. One method was to count the number of ions within a cylinder with an axis along the direction of impact and a radius of 10 Å. Alternatively (as in a plot given below) an angular deviation criterion could be considered. In the course of the work carried out here it was found that both criteria gave virtually identical results. In order to test to see whether a certain direction exhibited channelling, we launched the clusters at various angles relative to that direction. We did simulations in YIG ($Y_3Fe_2O_3$), counting the number of ions scattered by the end of the crystal to simulate standard back-scattering experiments. When the impact angle was sufficiently aligned with some major directions, we found that the number of scattered ions would drop significantly, indicating that channelling was taking place, see figure 1 where the

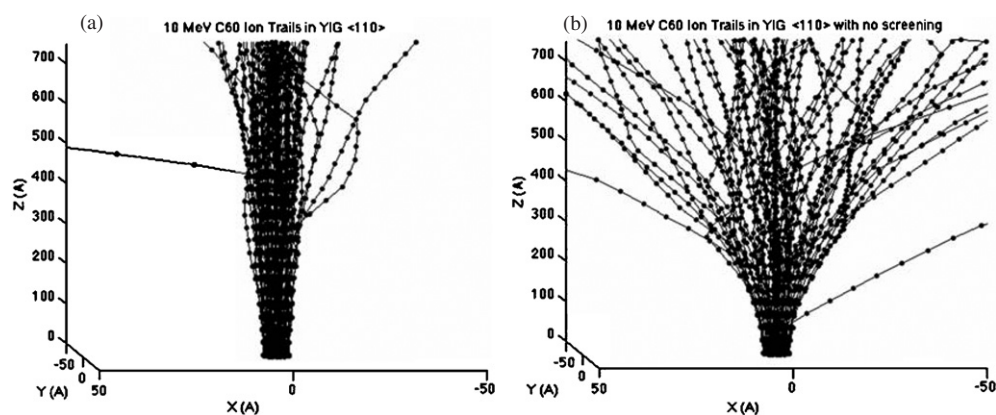


Figure 2. Plots tracing ion paths as they traverse the YIG lattice in the $\langle 110 \rangle$ direction, with the initial cluster energy of 10 MeV. The charge state of the ions throughout the channel is 1. (a) Screening length: 3 Å. (b) No Coulomb screening.

calculation was performed for the 10 MeV cluster for the $\langle 110 \rangle$ direction. The necessary alignment such that significant channelling was observed was usually only one or two degrees across. In other directions, such as the $\langle 111 \rangle$ direction in figure 1, the number of scattered ions remained the same across all the angles, indicating that channelling did not occur along those directions. Thus, one can clearly see the channelling effect in these diagrams, as opposed to non-channelling directions where scattering predominates in bringing about cluster breakup.

In order to ensure that these figures were not some artifact of the criteria used, and to do a sanity check on the simulation, we also found it useful to make 3D plots of the paths of each ion through the lattice. The resulting ‘brush plots’ allow a more qualitative but more comprehensive visualization of our results, see figure 2. In this figure, where we describe the interaction of a 10 MeV cluster along the $\langle 110 \rangle$ direction, we assumed that the ionic charge state is 1 throughout the entire cluster range, in accordance with the discussion above. We address here the question whether the 10 MeV cluster ions can provide enough Coulomb repulsion within the channel to disrupt the cluster substantially. Figure 2(a) describes the ‘brush plot’ assuming a screening length of 3 Å, less effective than the 1.5 Å calculated above for the YIG channel. The screening provided here, of 3 Å is sufficient to obtain cluster channelling. The ‘brush plot’ given in figure 2(b) describes the case of no screening of the Coulomb repulsion between cluster constituents. This ‘brush plot’ is very similar to that obtained for the $\langle 111 \rangle$ direction in figure 1 and indicates that channelling does not occur with no screening of the intra-cluster Coulomb potential.

We can also test to see how many of the ions are within an angular interval of 1.5° with respect to the initial cluster direction over time, in order to see how long the ions remained channelled, thereby employing the angular trapping definition. In figure 3 we describe simulations with 10 MeV clusters in YIG, assuming a charge state of 1 and a screening length of 3 Å, as in figure 2(a). We found that ions would stay together in channelling directions, orders of magnitude longer than in non-channelling directions. The directions $\langle 100 \rangle$, $\langle 010 \rangle$, $\langle 001 \rangle$ and $\langle 110 \rangle$ have large enough spacing between lattice atom strings in YIG that the ions remain trapped despite the Coulombic repulsion between them. The analysis of clusters incident on other major directions, $\langle 111 \rangle$, $\langle 211 \rangle$ and $\langle 753 \rangle$ showed that these directions acted more like homogeneous solids.

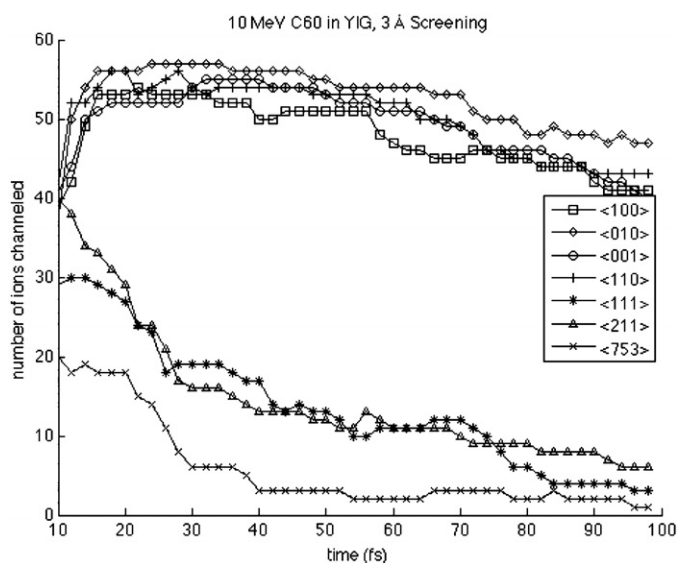


Figure 3. Counting the number of ions within 1.5° of the angle between the ion direction and the axis along the impact direction starting at the impact point, as the ions traverse the crystal. $\langle 100 \rangle$, $\langle 010 \rangle$, $\langle 001 \rangle$ and $\langle 110 \rangle$ exhibit channelling, while $\langle 111 \rangle$, $\langle 211 \rangle$ and $\langle 753 \rangle$ do not. Simulations were performed using a 10 MeV cluster in YIG, charge state 1 and a screening length of 3 Å.

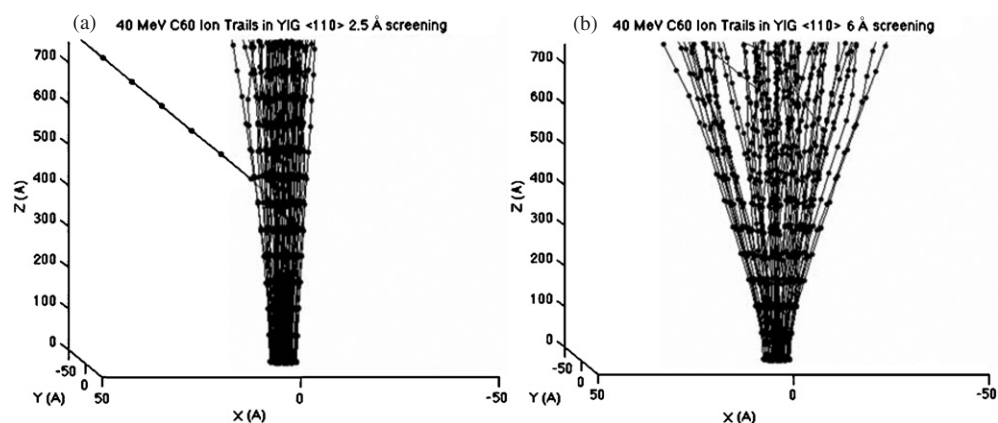


Figure 4. These brush plots show the effect of the screening length on channelling of high energy clusters. The plots are in the $\langle 110 \rangle$ direction in YIG with 40 MeV clusters. (a) has a 2.5 Å screening length, while (b) has a 6 Å screening length. The ionic charge state within the channel is 2.

In figure 4 we address whether the intra-cluster interaction can provide enough Coulomb repulsion within the channel to substantially disrupt the cluster in its motion through the channel, this time for the 40 MeV cluster. The cluster is launched again along the $\langle 110 \rangle$ direction, and in accordance with the discussion above with a charge state of 2 for each of the cluster constituents. In figure 4(a) we adopt the full screening as given by the screening length of 2.5 Å as calculated above for 40 MeV. In figure 4(b) the less effective screening length of

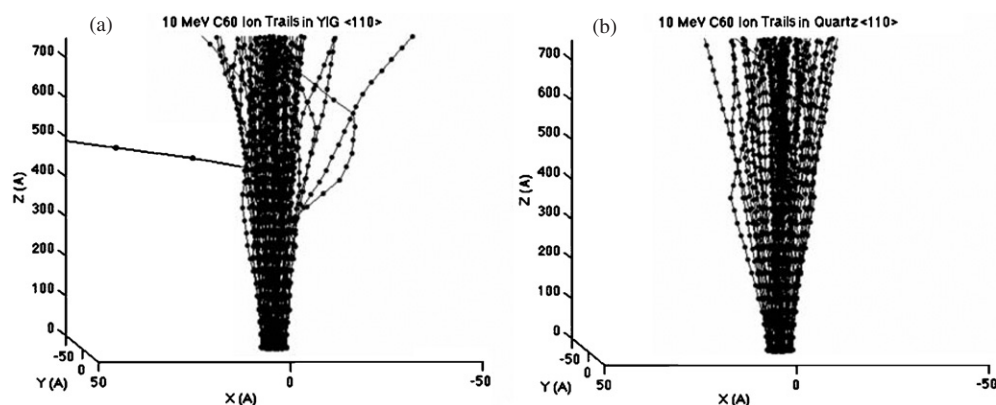


Figure 5. Plots tracing ion paths as they traverse the YIG lattice (a) compared to ions traversing alpha-quartz (b). These simulations are for 10 MeV clusters in the $\langle 110 \rangle$ direction with the screening length of 3 Å. The conditions here for YIG are identical to those of figure 2(a).

6 Å is assumed. These ‘brush plots’ indicate appreciable channelling for the 2.5 Å screening length, while for the 6 Å screening length the channelling is strongly diminished.

We have therefore observed, on the basis of figures 2 and 4, that channelling is dependent on the amount of screening of the intra-cluster Coulomb interaction. For the 10 MeV cluster, channelling is seen even for the ‘incomplete screening’ as given by the 3 Å screening length. Indeed, it would seem unlikely that in YIG, which is a dielectric material, all the valence electrons within the channel participate in the screening. For the 40 MeV cluster complete screening by all the valence electrons is needed to obtain channelling.

We also wanted to test our results from YIG in other crystal structures. On a qualitative level, results of the simulation with an α -quartz crystal lattice as the target were not significantly different from the YIG data. Channelling directions and non-channelling directions were the same, due to many similarities in the two crystal structures. The strings of trapping lattice atoms were further apart from those in YIG, but overall trends remained the same, see figure 5 where results for the 10 MeV cluster are plotted for both YIG and α -quartz. Since the α -quartz is composed of lighter atoms and a more simple crystal structure, it is reassuring that the results from YIG apply here, and likely that they are common to other lattices.

As the electron-wake phenomenon is relatively unstudied for such large clusters, we wanted to discover its direct effects on our simulation. It is expected to have a narrowing effect on the channelled ions, as the wakes of forward ions will pull those following towards the axis. This was beautifully demonstrated in a series of different experiments by Gemmell *et al* [15] for energetic small molecules. This effect however was found to be quite small and almost undetectable in our simulations of the channelled C₆₀ clusters.

In order to expedite comparisons of our simulations to expected experimental results, we also simulated the track damage one would observe. Using the energy deposition threshold in [16] of 0.178 eV Å⁻¹, we calculated energy deposition levels and plotted regions expected to be damaged (see figure 6 for the 10 MeV cluster). These predictions are reassuring. The channelling direction produces one solid track while the non-channelling direction produces forks and multiple smaller tracks. Unfortunately, there are many spurious regions marked as damaged that could not possibly be so, as they are smaller than the YIG cell size and so while the energy deposition threshold is met, it cannot sufficiently change the morphology of the crystal.

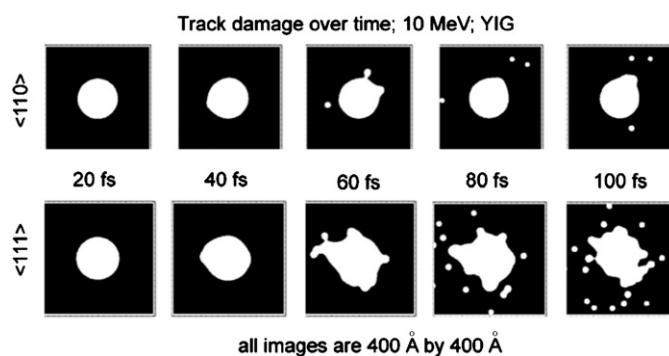


Figure 6. Expected track damage due to a 10 MeV cluster travelling in the channelling direction $\langle 110 \rangle$ and the non-channelling direction $\langle 111 \rangle$.

4. Discussion

As we have seen, we have been able to create a model of the channelling of ionic clusters in crystal lattices that may be useful in designing and interpreting experiments of the sort simulated here. This model is relatively mature and can handle a broad range of problems dealing with the interaction of clusters with crystalline targets as well with other targets such as nanotubes. We note that multiple scattering of the energetic ions by the free electron gas is not incorporated within the model. A very recent paper by Archubi and Arista [17] deals with this problem providing results for the channelling of protons through an 800 Å Au crystal. Scaling these results for carbon ions and for the less dense YIG channel, we obtain that the angular spread due to multiple scattering is not greater than 0.1° , essentially having no effect on the results presented here.

The model predicts here that for the 10 MeV C_{60} cluster, channelling occurs for a given range of initial directions along the crystalline axis, provided that intra-cluster screening exists, although the full amount of screening which could be provided by the valence electrons is not needed. For the 40 MeV C_{60} cluster, the same is true provided the Coulomb interaction between the ions is fully screened by the valence electrons within the channel, which might not occur for the dielectric materials considered here but probably would for a conducting solid.

The specific results of the simulations presented here are strongly dependent on the values of the ionic charge state as well as on the dynamic screening of the electron gas within the channel. Both of these are detrimental for the explosion of the cluster and were determined making simplified physical assumptions. Because of this, we have used charge state values that should reflect an underestimation of the channelling phenomenon. In this connection it would be of great interest to measure the charge state of channelled individual carbon ions in this low-energy region, for different crystalline targets. Experimental studies on the type of systems simulated here, using targets of different dielectric character, in tandem with the individual charge state experiment would shed light on the screening problem.

Finally, there are a few improvements that could make this model more descriptive of the relevant physics, however, that requires more study. It is our hope that this model and the results shown here will be an incentive for further experimental work on cluster ion-induced channelling and track damage, using targets of different dielectric characters, and with different cluster energies and sizes.

References

- [1] Krause H F and Datz S 1996 *Adv. At. Mol. Opt. Phys.* **37** 139
- [2] Dunlop A, Jaskierowicz G, Jensen J and Della-Negra S 1997 *Nucl. Instrum. Methods Phys. Res. B* **132** 93
- [3] Le Beyec Y 2000 Private communication
- [4] Hartman J W, Tombrello T A, Bouneau S, Della-Negra S, Jacquet D, Le Beyec V and Pautrat M 2000 *Phys. Rev. A* **62** 043202
- [5] Hartman J W 1997 Simulation of surface and material damage during fast ion penetration *PhD Thesis*, California Institute of Technology
- [6] Biersack J P and Haggmark L G 1980 *Nucl. Instrum. Methods Phys. Res.* **174** 257
- [7] Ziegler J F, Biersack J B and Littmark U 1985 *The Stopping and Range of Ions in Solids* (Oxford: Pergamon)
- [8] Jishi R A, Mirie R M and Dresselhaus M S 1992 *Phys. Rev. B* **45** 13685
- [9] Andriamonje S *et al* 1989 *Phys. Rev. Lett.* **63** 1930
- [10] Bentini G G, Albertazzi E, Bianconi M, Lotti R and Lulli G 2002 *Nucl. Instrum. Methods Phys. Res. B* **193** 113
- [11] Andersen J U *et al* 1993 *Phys. Rev. Lett.* **70** 750
- [12] Brunelle A, Della Negra S, Depauw J, Jacquet D, Le Beyec Y and Pautrat M 1999 *Phys. Rev. A* **59** 4456
- [13] Nardi E and Tombrello T A 2006 *J. Phys.: Condens. Matter* **18** 11357
- [14] Fisher D V, Henis Z, Eliezer S and Meyer-Ter-Vehn J 2006 *Laser Part. Beams* **24** 81
- [15] Gemmell D S, Remillieux J, J-C Poizat, Gaillard M J, Holland R E and Vager Z 1975 *Phys. Rev. Lett.* **34** 1420
- [16] Tombrello T A, Childs A M and Hartman J W 1998 *Nucl. Instrum. Methods Phys. Res. B* **145** 429
- [17] Archubi C D and Arista N A 2006 *Phys. Rev. A* **74** 052717